



HAL
open science

A Boundary Observer for Two Phase Heat Exchangers

Mohammad Ghousein, Emmanuel Witrant

► **To cite this version:**

Mohammad Ghousein, Emmanuel Witrant. A Boundary Observer for Two Phase Heat Exchangers. ECC 2019 - 18th European Control Conference, Jun 2019, Naples, Italy. pp.2332-2337, 10.23919/ECC.2019.8796247 . hal-03511211

HAL Id: hal-03511211

<https://hal.univ-grenoble-alpes.fr/hal-03511211>

Submitted on 4 Jan 2022

HAL is a multi-disciplinary open access archive for the deposit and dissemination of scientific research documents, whether they are published or not. The documents may come from teaching and research institutions in France or abroad, or from public or private research centers.

L'archive ouverte pluridisciplinaire **HAL**, est destinée au dépôt et à la diffusion de documents scientifiques de niveau recherche, publiés ou non, émanant des établissements d'enseignement et de recherche français ou étrangers, des laboratoires publics ou privés.

A Boundary Observer for Two Phase Heat Exchanger*

Mohammad Ghousein and Emmanuel Witrant

Abstract—In this work, we consider the estimation of the thermodynamic properties (Pressure, Enthalpy, Temperature) and mass flow rates along the pipes of a concentric heat exchanger tube in which we have CO₂ as the working refrigerant. The transport phenomena are modeled using Navier-Stokes equations in 1D for both hot and cold sides, where we consider single and two phase flows. The estimation is done with a PDE observer that uses measurements taken at the tube boundaries to construct the required profiles along the tubes. The convergence of this observer is proved using Lyapunov analysis and the theoretical results are illustrated by numerical simulations.

I. INTRODUCTION

Heat exchangers are devices used to exchange energy between fluids. They are part of any refrigeration (cooling or heating) cycle and they are used in many industrial domains like food production, chemical plants, oil refineries, etc.. The basic motivation of this work is the cooling of the silicon detectors at CERN. In fact, the new generation cooling systems for detector applications have a reduced mass and include significant cost reduction in the areas of maintenance, repair, and overall operating costs. Recent studies (see e.x. [1]) show that evaporative CO₂ cooling is ideal for this purpose as they need smaller tubes than conventional systems. Also, in comparison with fluoro-carbons (C₂F₆, C₃F₈, R134a) refrigerants, CO₂ seems to have the high heat transfer capability which is extremely important from an energy management point of view. CO₂ itself is a greenhouse gas, however, studies show that the impact of HFCs on global warming is up to 6,000 times higher than CO₂. Thus, the idea of using CO₂ in cooling is now developing.

We consider a concentric tube CO₂ heat exchanger as the evaporator system. Energy flows from the inner tube (hot liquid CO₂ fluid) to the outer tube (cold two-phase liquid+gas CO₂ fluid) through the wall interface. The two-phase physical state is characterized by the change of density of the moving flow while keeping its saturation temperature approximately constant. The control and supervision of such refrigeration unit is vital in order to have low energy consumption rates while maximizing the heat transfer rates. However, the evaporation phenomenon complicates the physical modeling since the full nonlinear conservation equations (mass, momentum and energy conservations) are considered, with the presence of time varying transport speeds and

uncertain heat transfer and friction coefficients. In addition, states measurements are only available at the inlet and outlet of the tubes while the full distributed state may be required by the designed control law. For this purpose, we build a boundary observer that reconstructs the thermodynamic profile (enthalpy, pressure, mass flow rate) for each flow by only measuring the thermodynamical states at the extremities of the system.

The transport phenomena and the exchange of heat on both hot and cold sides is modeled using 1D Navier-Stokes equations. Our system then falls into the category of nonlinear hyperbolic systems of balance laws. Engineering solutions to the estimation problem is to discretize the system of PDEs and then to use classical methods for finite dimensional systems. However, in this case, vital information on the system transient behavior is lost and the observability and the controllability depend on the chosen discretization method. This motivates us to extend the finite dimensional control theory to the infinite case.

Hyperbolic systems are widely investigated in the control community since they can model a wide class of physical systems with important real applications (see e.g. Chapter 1 in [2]). Practically, boundary control and boundary observation of such systems is more realistic than distributed control since actuators and sensors are usually placed at the extremities of the domain. The reader can find complete results on boundary controllability and observability of quasilinear hyperbolic systems in the book of [3]. Concerning boundary control design, the authors in [2] dedicated an entire volume to the study of boundary stabilization of 1D hyperbolic systems using dissipative boundary conditions (standard static boundary output feedback). The main stability analysis is based on choosing feedback gains that ensure exponential convergence of a quadratic Lyapunov functional. Furthermore, backstepping boundary control design is extensively addressed in the literature for hyperbolic systems. The main idea of this method is the introduction of an invertible Volterra transformation that maps the original system into a target system with the desired stability properties (see e.g. [4], [5], [6], [7]).

Boundary observers for hyperbolic systems are less investigated in the literature. In [4], a boundary controller-observer is designed for a 2×2 coupled linear hyperbolic system with spatially varying coefficients using a backstepping approach. Similar ideas for the general system can be found in [6] and [7]. On the other hand, using a different and simpler method, the authors in [8] designed a boundary observer for n rightward convecting hyperbolic equations. The exponential convergence of this observer is proved using a

*This work was sponsored within the ITEA3 European project, 15016 EMPHYSIS (Embedded systems with physical models in the production code software).

The authors are with Control Systems Department, GIPSA-lab, Grenoble, France. E-mails: {mohammad.ghousein, emmanuel.witrant}@gipsa-lab.fr

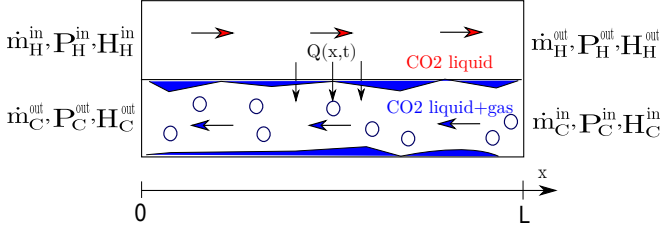


Fig. 1. CO₂ two phase heat exchanger

strict Lyapunov candidate. This result is extended by the authors in [9] to one rightward and one leftward transport PDEs for the plate heat exchanger. In this framework, our contribution is a complete boundary state estimation of the thermodynamic profile (pressure, enthalpy, mass flow rate) along the length of a CO₂ heat exchanger built using concentric tubes that contain two-phase flows. The system is modeled by three transport equations (mass, momentum and energy) for both the hot and cold sides in order to capture the necessary transients of the two phase regime. The equations are then linearized around a chosen steady state in the working ranges of interest. For the observer design, we get the inspiration from [9], extended to the case of three rightward and three leftward transport PDEs. Sufficient conditions for the exponential convergence of the observer are derived in form of a linear matrix inequality (LMI) and a bilinear one by using a Lyapunov functional used in [10]. The paper is organized as follows: the problem description is given in Section II, providing the physical model of the two phase flows. The observer design with the estimation convergence analysis is presented in Section III. Section IV is dedicated to the simulation results for a toy model of a two phase heat exchanger, where we address the robustness of the observer to measurement noises. Some concluding remarks are given in Section V.

II. PROBLEM DESCRIPTION

We consider the concentric tube heat exchanger shown in Fig.1. This exchanger is a counter flow heat exchanger in which hot and cold fluids flow in opposite directions to maximize the heat transfer. The hot fluid enters in liquid phase and leaves in liquid phase while the cold fluid enters in two phase and leaves in two phase. The flow of heat $Q(x,t)$ is from the hot side to cold side through the wall interface. The subscripts *in/out* denote inflow and outflow directions and the superscripts *H* and *C* refer to the hot and cold channels. The mathematical model is derived based on the following assumptions:

- the flow is 1-D unidirectional (the hot fluid flows in the positive x direction);
- the two phase flow is homogeneous i.e. liquid and gas flow at the same velocity and they are in thermodynamic equilibrium;
- the kinetic and potential energies of the flows entering and leaving the tubes are neglected;

TABLE I
DEFINITION OF THE SYSTEM VARIABLES AND CONSTANTS. $K = C$ (COLD FLUID), $K = H$ (HOT FLUID)

Symbol	Description	Unit
ρ_k	Density	Kg/m ³
P_k	Pressure	Pa
H_k	Specific Enthalpy	J/Kg
\dot{m}_k	Mass flow rate	Kg/s
T_k	Temperature	K
α	Overall heat transfer coefficient	W/m ² ·K
A_k	Tube cross-sectional area	m ²
L	Heat exchanger length	m
D_1, D_H	Inner,hydraulic tube diameter respectively	m
f_k	Friction coefficient	-

- the wall thickness is neglected (no wall dynamics) and the heat transfer and friction coefficients are constant and uniform;
- the heat exchanger is perfectly isolated and does not exchange heat with its surrounding environment;

Based on the above assumptions, the heat exchanger dynamics can be described by a set of first order hyperbolic partial differential equations of balance laws (mass, momentum and energy conservation) as follows, $\forall x \in [0, 1]$ (normalized space):

- *cold flow (two phase)*:

$$A_C \frac{\partial \rho_C}{\partial t} - \frac{1}{L} \frac{\partial \dot{m}_C}{\partial x} = 0 \quad (1)$$

$$\frac{\partial \dot{m}_C}{\partial t} - \frac{1}{L} \frac{\partial}{\partial x} \left(\frac{\dot{m}_C^2}{\rho_C A_C} \right) - \frac{A_C}{L} \frac{\partial P_C}{\partial x} + \frac{f_C \dot{m}_C |\dot{m}_C|}{2D_H \rho_C A_C} = 0 \quad (2)$$

$$A_C \frac{\partial (\rho_C H_C - P_C)}{\partial t} - \frac{1}{L} \frac{\partial (\dot{m}_C H_C)}{\partial x} = \pi D_1 \alpha (T_H - T_C) \quad (3)$$

- *hot flow (single phase)*:

$$A_H \frac{\partial \rho_H}{\partial t} + \frac{1}{L} \frac{\partial \dot{m}_H}{\partial x} = 0 \quad (4)$$

$$\frac{\partial \dot{m}_H}{\partial t} + \frac{1}{L} \frac{\partial}{\partial x} \left(\frac{\dot{m}_H^2}{\rho_H A_H} \right) + \frac{A_H}{L} \frac{\partial P_H}{\partial x} + \frac{f_H \dot{m}_H |\dot{m}_H|}{2D_1 \rho_H A_H} = 0 \quad (5)$$

$$A_H \frac{\partial (\rho_H H_H - P_H)}{\partial t} + \frac{1}{L} \frac{\partial (\dot{m}_H H_H)}{\partial x} = -\pi D_1 \alpha (T_H - T_C) \quad (6)$$

where the definition of all equations variables is given in Table I.

Remark 1: We model the two-phase and single-phase flows in the same way, ((1)-(3) are similar to (4)-(6)). The reason is that CO₂ in two-phase state has an important characteristic: the ratio of liquid density to vapor density (ρ_l/ρ_v) is small [11], this results in a homogeneous two phase dynamics similar to the single-phase dynamics. However, the difference is in the calculation of thermodynamic properties for each flow e.g. for two phase flows we have the concept of quality q ($0 \leq q \leq 1$):

$$q = \frac{H_C - H_l^{sat}}{H_v^{sat} - H_l^{sat}}$$

which is the ratio of liquid to vapor mass in a two phase flow, H_l^{sat} and H_v^{sat} are the enthalpies of CO₂ in the saturated liquid and saturated vapor states respectively.

Most refrigeration cycles are studied on a Pressure-Enthalpy diagram (P-H diagram); i.e. by knowing the pressure and enthalpy of a fluid at time t , all the other thermodynamic variables (temperature, density, quality, etc..) can be calculated by an equation called the Equation of State (EoS). Considering:

$$W = [\dot{m}_H, P_H, H_H, \dot{m}_C, P_C, H_C]^T$$

as the state of system (1)-(6), we complete the model (1)-(6) by the following equations of state for temperature and density:

$$T_k = f_k(P_k, H_k) \quad (7)$$

$$\rho_k = g_k(P_k, H_k) \quad (8)$$

where $k = C$ or $k = H$. The functions f_k and g_k are approximated by first order Taylor expansion around the points of saturation P_k^{sat}, H_k^{sat} in the working ranges of interest for the pressure. These points (P_k^{sat}, H_k^{sat}) correspond to the saturated liquid state of the CO₂ fluid.

The system (1)-(6) has boundary conditions of the following form

$$\begin{aligned} W_1(1, t) &= \dot{m}_H^{out}(t), & W_4(0, t) &= \dot{m}_C^{out}(t) \\ W_2(0, t) &= P_H^{in}(t), & W_5(1, t) &= P_C^{in}(t) \\ W_3(0, t) &= H_H^{in}(t), & W_6(1, t) &= H_C^{in}(t) \end{aligned} \quad (9)$$

and the initial conditions:

$$W(x, 0) = W_0(x) \quad (10)$$

Synthesizing a distributed control law requires the complete profile (P, H, \dot{m}) along the channels of the exchanger, i.e we need to have access to these values at any instant and at each position in space. This requires to place sensors at each position which is costly and inefficient. A more reasonable locations for the sensors is at the boundaries of the tubes. As a result, we assume that we have all the input/output measurements at the extremities (see Fig.1) and our objective is to estimate the profile (P, H, \dot{m}) along the total length.

III. OBSERVER DESIGN

We first consider the linearization of (1)-(10) around the steady state $W_S(x)$, such that:

$$W(x, t) = W_S(x) + \Delta W(x, t) \quad (11)$$

Using a Taylor expansion of order 1 we get the following dynamics of the infinitesimal state $\Delta W(x, t)$:

$$\partial_t \Delta W + A_S(x) \partial_x \Delta W + B_S(x) \Delta W = 0 \quad (12)$$

where $A_S(x), B_S(x)$ are $\mathcal{M}_{6,6}(\mathbb{R})$ steady-state matrices whose entries are given in Appendix V. While our method is still applicable with space-varying matrices, we take the average value of the matrices $A_S(x), B_S(x)$ over the hole domain $[0, 1]$

just for the sake of technical simplicity in the calculations, We then have that:

$$\partial_t \Delta \bar{W} + \bar{A}_S \partial_x \Delta \bar{W} + \bar{B}_S \Delta \bar{W} = 0 \quad (13)$$

where \bar{A}_S and \bar{B}_S are the average values of $A_S(x)$ and $B_S(x)$, respectively. The state $\Delta \bar{W}$ corresponds to the system (12) with space-averaged matrices. Using (11), system (13) has the following perturbed boundary conditions

$$\begin{aligned} \Delta \bar{W}_1(1, t) &= \Delta \dot{m}_H^{out}(t), & \Delta \bar{W}_4(0, t) &= \Delta \dot{m}_C^{out}(t) \\ \Delta \bar{W}_2(0, t) &= \Delta P_H^{in}(t), & \Delta \bar{W}_5(1, t) &= \Delta P_C^{in}(t) \\ \Delta \bar{W}_3(0, t) &= \Delta H_H^{in}(t), & \Delta \bar{W}_6(1, t) &= \Delta H_C^{in}(t) \end{aligned} \quad (14)$$

with initial conditions

$$\Delta \bar{W}(0, x) = \Delta \bar{W}^0(x) \quad (15)$$

We know from the physics of the system that the matrix \bar{A}_S is diagonalizable and it has 6 eigen-values (3 positive and 3 negative), since for each fluid we have mass and energy flow in one direction and momentum in the reverse direction (see e.x. [12]). As a result, system (13)-(15) is hyperbolic. The controllability and observability of such system has been proved in [3], hence we can build a boundary observer to estimate the distributed thermodynamic profiles.

A. Observer architecture

We start by transforming the system (13)-(15) into the characteristic form using a linear transformation T :

$$\Delta \bar{W} = T \Delta Z, \quad \Lambda = T^{-1} \bar{A}_S T, \quad \Sigma = T^{-1} \bar{B}_S T \quad (16)$$

where $\Lambda = \text{diag}\{\lambda_1 \dots \lambda_6\}$ and Σ is arbitrary, where $(\lambda_1 > 0, \lambda_3 > 0, \lambda_5 > 0)$ and $(\lambda_2 < 0, \lambda_4 < 0, \lambda_6 < 0)$. Equation (13) can then be written as:

$$\partial_t \Delta Z + \Lambda \partial_x \Delta Z + \Sigma \Delta Z = 0 \quad (17)$$

Let us introduce the following notation:

$$\Delta Z = (\Delta Z^+(x, t), \Delta Z^-(x, t))$$

where $\Delta Z^+ = (\Delta Z_1, \Delta Z_3, \Delta Z_5)$ and $\Delta Z^- = (\Delta Z_2, \Delta Z_4, \Delta Z_6)$. The boundary conditions are transformed by (16) to the following form

$$\Delta Z^+(0, t) = M_1 \Delta Z^-(0, t) + N_1 F_1(t) \quad (18)$$

$$\Delta Z^-(1, t) = M_2 \Delta Z^+(1, t) + N_2 F_2(t) \quad (19)$$

where M_1, M_2, N_1, N_2 are $\mathcal{M}_{3,3}(\mathbb{R})$ calculated using the transformation T and $F_1(t) = (\Delta P_H^{in}, \Delta H_H^{in}, \Delta \dot{m}_C^{out})^T$, $F_2(t) = (\Delta P_C^{in}, \Delta H_C^{in}, \Delta \dot{m}_H^{out})^T$ are the vectors of inputs. System (17) has the following unknown initial conditions

$$\Delta Z(x, 0) = \Delta Z_0(x) \quad (20)$$

Our aim is to build the observer on the transformed dynamics ΔZ and then use the transformation T to construct the estimated state for $\Delta \bar{W}$. Denote by $\Delta \hat{Z}$ the estimated state of ΔZ . Considering that only boundary measurements are available i.e. $y_1(t) = \Delta Z^-(0, t)$ and $y_2(t) = \Delta Z^+(L, t)$, a

natural choice for the observer design is to set the dynamics of the estimator as, $\forall x \in [0, 1]$:

$$\partial_t \Delta \hat{Z} + \Lambda \partial_x \Delta \hat{Z} + \Sigma \Delta \hat{Z} = 0 \quad (21)$$

with boundary conditions:

$$\begin{aligned} \Delta \hat{Z}^+(0, t) &= M_1 \Delta Z^-(0, t) + N_1 F_1(t) \\ &\quad - 1_{3 \times 3} L^- (\Delta \hat{Z}^-(0, t) - y_1(t)) \end{aligned} \quad (22)$$

$$\begin{aligned} \Delta \hat{Z}^-(1, t) &= M_2 \Delta Z^+(1, t) + N_2 F_2(t) \\ &\quad - 1_{3 \times 3} L^+ (\Delta \hat{Z}^+(1, t) - y_2(t)) \end{aligned} \quad (23)$$

The inflow boundary conditions are thus corrected by the error of the outflows boundaries, and the same is done for the outflow observer boundaries, which are corrected by the errors of the inflow boundaries. All the errors are weighted by the observer gains $L^+ = \text{diag}\{L_1, L_3, L_5\}$ and $L^- = \text{diag}\{L_2, L_4, L_6\}$. $1_{3 \times 3}$ is the 3 by 3 ones matrix.

B. Global Exponential Stability (GES)

In this section, we prove the global exponential convergence of the observer (21) with boundary conditions (22)-(23). This is done by proving the exponential convergence of the estimated error $\varepsilon(x, t) = \Delta Z(x, t) - \Delta \hat{Z}(x, t)$ towards zero. Let us start by considering the error dynamics:

$$\partial_t \varepsilon + \Lambda \partial_x \varepsilon + \Sigma \varepsilon = 0 \quad (24)$$

with the following boundary conditions:

$$\begin{aligned} \varepsilon^+(0, t) &= -1_{3 \times 3} L^- \varepsilon^-(0, t) \\ \varepsilon^-(1, t) &= -1_{3 \times 3} L^+ \varepsilon^+(1, t) \end{aligned} \quad (25)$$

Definition 1: System (24)-(25) is said to be *Globally Exponentially Stable* if there exist $\gamma > 0$ and $C > 0$ such that for every initial condition $\varepsilon^0 \in L^2((0, 1); \mathbb{R}^6)$ the solution of the system (24)-(25) satisfies:

$$\|\varepsilon(t, \cdot)\|_{L^2((0, 1); \mathbb{R}^6)} \leq C e^{-\gamma t} \|\varepsilon^0\|_{L^2((0, 1); \mathbb{R}^6)} \quad (26)$$

The GES of (24)-(25) can be inferred from the following theorem.

Theorem 1: Consider the system of PDEs (24) with boundary conditions (25). Suppose that there exist $\gamma > 0$, $\mu \in \mathbb{R}$, a positive definite matrix $Q(x) > 0$ and observer gains L^+ and L^- such that for all $x \in [0, 1]$ we have:

$$\begin{aligned} \Sigma^T |\Lambda|^{-1} Q(x) + |\Lambda|^{-1} Q(x) \Sigma - 2\mu Q(x) &\leq -2\gamma |\Lambda|^{-1} Q(x) \\ \left(\begin{array}{cccccc} -q_2^0 + \alpha L_2^2 & \alpha L_2 L_4 & \alpha L_2 L_6 & 0 & 0 & 0 \\ * & -q_4^0 + \alpha L_4^2 & \alpha L_4 L_6 & 0 & 0 & 0 \\ * & * & -q_6^0 + \alpha L_6^2 & 0 & 0 & 0 \\ 0 & 0 & 0 & -q_1^1 + \beta L_1^2 & \beta L_1 L_3 & \beta L_1 L_5 \\ 0 & 0 & 0 & * & -q_3^1 + \beta L_3^2 & \beta L_3 L_5 \\ 0 & 0 & 0 & * & * & -q_5^1 + \beta L_5^2 \end{array} \right) &\leq 0 \end{aligned} \quad (27)$$

where q_i^0 and q_i^1 for $i \in \{1, \dots, 6\}$ are the diagonal entries of $Q(0)$ and $Q(1)$, respectively, $\alpha = q_1^0 + q_3^0 + q_5^0$ and $\beta = q_2^1 + q_4^1 + q_6^1$.

Then system (24) with (25) is (GES).

Proof 1: Consider the following Lyapunov candidate, similar to the one used in [10]:

$$V(\varepsilon) = \int_0^1 \varepsilon^T(x) |\Lambda|^{-1} Q(x) \varepsilon(x) dx \quad (29)$$

where $\mu > 0$, $|\Lambda|^{-1} = \text{diag}\{1/|\Lambda_i|\}$ and $Q(x) = \text{diag}\{q_i e^{-\text{sign}(\Lambda_i) 2\mu x}\}$ for all $i \in \{1, \dots, 6\}$.

Taking the time derivative of (29) we have:

$$\begin{aligned} \dot{V} &= \int_0^1 \partial_t \varepsilon^T |\Lambda|^{-1} Q(x) \varepsilon dx + \int_0^1 \varepsilon^T |\Lambda|^{-1} Q(x) \partial_t \varepsilon dx \\ &= \int_0^1 (\varepsilon^T \Sigma^T - \partial_x \varepsilon^T \Lambda^T) |\Lambda|^{-1} Q(x) \varepsilon dx + \\ &\quad \int_0^1 \varepsilon^T |\Lambda|^{-1} Q(x) (\Sigma \varepsilon - \Lambda \partial_x \varepsilon) dx \\ &= \int_0^1 \varepsilon^T \Sigma^T |\Lambda|^{-1} Q(x) \varepsilon dx + \int_0^1 \varepsilon^T |\Lambda|^{-1} Q(x) \Sigma \varepsilon dx \\ &\quad - \int_0^1 \partial_x \varepsilon^T \Lambda^T |\Lambda|^{-1} Q(x) \varepsilon + \varepsilon^T |\Lambda|^{-1} Q(x) \Lambda \partial_x \varepsilon dx \end{aligned}$$

Noting that $|\Lambda|^{-1} Q(x) = Q(x) |\Lambda|^{-1}$ and $|\Lambda|^{-1} \Lambda = \check{I}_6 = \text{diag}[\text{sign}(\Lambda_i)]$, then

$$\begin{aligned} \dot{V} &= \int_0^1 \varepsilon^T \Sigma^T |\Lambda|^{-1} Q(x) \varepsilon + \varepsilon^T |\Lambda|^{-1} Q(x) \Sigma \varepsilon dx - \\ &\quad \int_0^1 \partial_x \varepsilon^T \check{I}_6 Q(x) \varepsilon + \varepsilon^T \check{I}_6 Q(x) \partial_x \varepsilon dx \end{aligned} \quad (30)$$

Using the expansion: $\partial_x (\varepsilon^T \check{I}_6 Q(x) \varepsilon) = \partial_x \varepsilon^T \check{I}_6 Q(x) \varepsilon + \varepsilon^T \check{I}_6 Q(x) \partial_x \varepsilon + \varepsilon^T \check{I}_6 \partial_x (Q(x)) \varepsilon$ implies that

$$\begin{aligned} \dot{V} &= \underbrace{-[\varepsilon^T \check{I}_6 Q(x) \varepsilon]_0^1}_{\leq 0} \\ &\quad + \int_0^1 \varepsilon^T \underbrace{(\Sigma^T |\Lambda|^{-1} Q(x) + |\Lambda|^{-1} Q(x) \Sigma - 2\mu Q(x))}_{\leq -2\gamma |\Lambda|^{-1} Q(x)} \varepsilon dx \end{aligned} \quad (31)$$

The constraints (27) and (28) guarantee that $\dot{V} \leq -2\gamma V$ and for $t \in \mathbb{R}^+$ we have $V(\varepsilon(t, \cdot)) \leq e^{-2\gamma t} V(\varepsilon^0)$. To finalize the proof, equation (29) implies that:

$$\lambda_{\min} |\varepsilon|_{L^2((0, 1); \mathbb{R}^6)}^2 \leq V(\varepsilon) \leq \lambda_{\max} |\varepsilon|_{L^2((0, 1); \mathbb{R}^6)}^2 \quad (32)$$

where $(\lambda_{\min}, \lambda_{\max})$ are the minimum and maximum Eigen values of the matrix $(|\Lambda|^{-1} Q(x))$ for all $x \in [0, 1]$, respectively. We obtain the GES since:

$$\begin{aligned} \lambda_{\min} |\varepsilon|_{L^2((0, 1); \mathbb{R}^6)}^2 &\leq e^{-2\gamma t} V(\varepsilon^0) \leq \lambda_{\max} e^{-2\gamma t} |\varepsilon^0|_{L^2((0, 1); \mathbb{R}^6)}^2 \\ \Leftrightarrow |\varepsilon|_{L^2((0, 1); \mathbb{R}^6)} &\leq \sqrt{\frac{\lambda_{\max}}{\lambda_{\min}}} e^{-\gamma t} |\varepsilon^0|_{L^2((0, 1); \mathbb{R}^6)} \end{aligned} \quad (33)$$

which implies (26) and completes the proof.

IV. SIMULATION RESULTS

The performance of the proposed observer architecture is evaluated by comparing the output of the system's model along with the results of the observer simulation. The validation scenario is done in the following order:

- 1) The nonlinear model (1)-(8) is simulated using the finite volume method under constant boundary conditions with toy values for the exchanger dimensions, heat transfer coefficient and friction coefficients. All the values are given in Table II:

TABLE II
NONLINEAR MODEL PARAMETERS

$L = 18$ m	$D_1 = 12$ mm	$D_2 = 33.4$ mm
$f_H = 15$	$f_C = 30$	$\alpha = 100$ W/m ² ·K
$W_1(1,t) = 0.02$ Kg/s	$W_2(0,t) = 3$ MPa	$W_3(0,t) = 3$ KJ/Kg
$W_4(0,t) = 0.02$ Kg/s	$W_5(1,t) = 2.2$ MPa	$W_6(1,t) = 200$ KJ/Kg

- 2) Once the system (1)-(8) has reached the steady state $W^S(x)$, the linearized averaged matrices \bar{A}_S and \bar{B}_S are calculated by averaging $A^S(x)$ and $B^S(x)$ (see appendix V) over the whole domain.
- 3) The matrices Λ and Σ are constructed using the transformation T in (16), then (27) is solved using the polytopic approach proposed by [10] to find the matrix $Q(x)$. The equation is solved for $\mu = 1.05$ and $\gamma = 10^{-4} \text{ s}^{-1}$
- 4) The bilinear Matrix Inequality (BMI) (28) is solved by first ensuring that the diagonal elements are negative and then adjust the gains to satisfy the BMI. The values obtained are: $L_1 = 0.0092$, $L_2 = 0.3276$, $L_3 = 0.0104$, $L_4 = 0.2141$, $L_5 = 0.0058$ and $L_6 = 0.3943$

After calculating all the parameters, we are in a position to perform the simulation. We present here the worst case scenario, i.e. the observer is simulated using far initial conditions (linearization still valid) from the model with the addition of additive Gaussian noises (signal to noise ratio SNR=100) to the boundary measurements. We start the model at the steady state $W^S(x)$ then we do a step decrease of 15 KJ/Kg in the inlet hot enthalpy at $T = 1000$ s. The observer is started at the following initial conditions:

$$\hat{W}_0(x) = W^S(x) + \Delta \hat{W}^0(x)$$

where the values of $\Delta \hat{W}^0(x)$ are: $\Delta \hat{W}_1^0(x) = 10^{-3}$, $\Delta \hat{W}_2^0(x) = 50$ KJ/Kg, $\Delta \hat{W}_3^0(x) = 0.15$ MPa, $\Delta \hat{W}_4^0(x) = 10^{-3}$ Kg/s, $\Delta \hat{W}_5^0(x) = 50$ KJ/Kg and $\Delta \hat{W}_6^0(x) = 0.15$ MPa.

The simulated response is shown on Fig. 2 to 6. We can see that the observer converges with some initial oscillations despite of the measurements noises and far initial conditions. We clearly observe on Fig.6 the convergence of the estimation error to a minimum value determined by the noise amplitude. The measurements noises are attenuated and we can conclude that the proposed observer is reasonably robust.

V. CONCLUSIONS

We have proposed a boundary observer for the two phase heat exchanger. The observer was built on the linearized dynamics of the 1D Navier-Stokes equations assuming constant

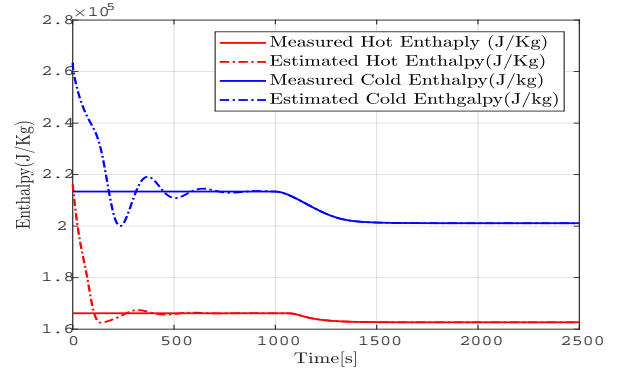


Fig. 2. Output Enthalpy.

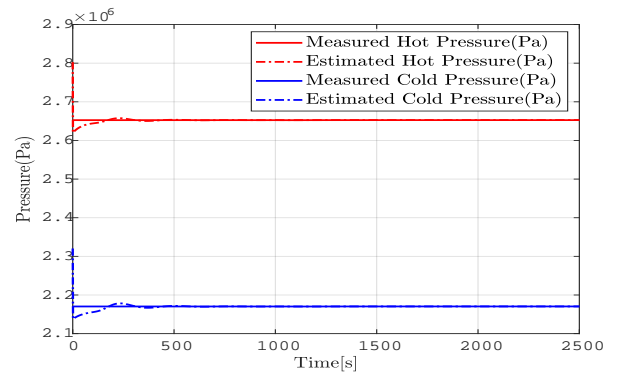


Fig. 3. Output Pressure.

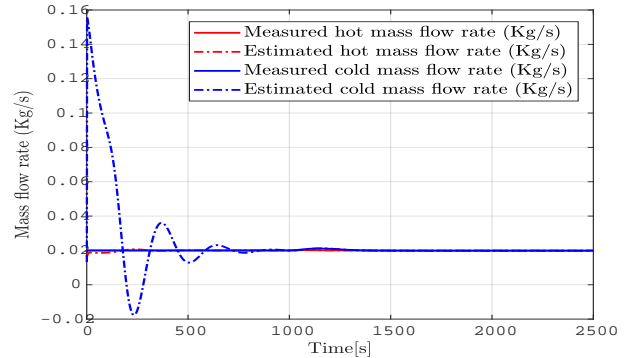


Fig. 4. Input Mass Flow Rate.

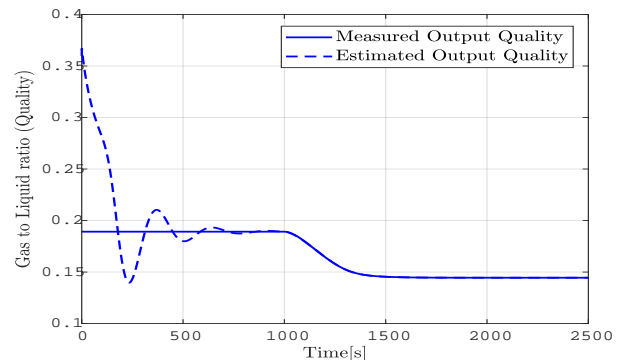


Fig. 5. Output Quality.

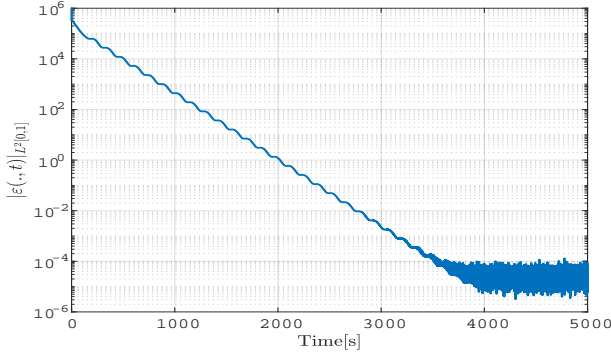


Fig. 6. L^2 norm of the error ϵ

heat transfer and friction coefficients. A Lyapunov approach was used to derive sufficient conditions for the exponential convergence of the estimation error and to calculate the observer gains. An important future work for us is to consider state dependent heat and friction coefficients, this is more realistic specially when considering two phase flows. Another interesting work would be to extend this approach to quasilinear hyperbolic PDEs.

APPENDIX

Consider approximating the non-differentiable function absolute ($\text{abs}(x)$) in the momentum equations (2)-(5) by a differentiable function $|x| \approx \sqrt{x^2 + \epsilon}$ for a very small $\epsilon > 0$, the nonlinear system (1)-(8) is linearized using first order Taylor expansion around $W^S(x)$ and we have the following steady state matrices:

- $A_1^S(x)$ is $\mathcal{M}_{6,6}(\mathbb{R})$ with all zeros except the entities:
 $a_{12} = A_H(\frac{\partial \rho}{\partial P}|_H)_H$, $a_{13} = A_H(\frac{\partial \rho}{\partial h}|_P)_H$, $a_{32} = -A_H$,
 $a_{21} = 1$, $a_{33} = A_H \rho_H$, $a_{45} = A_C(\frac{\partial \rho}{\partial P}|_C)_C$,
 $a_{46} = A_C(\frac{\partial \rho}{\partial h}|_P)_C$, $a_{54} = 1$, $a_{65} = -A_C$, $a_{66} = A_C \rho_C$.
- $B_1^S(x)$ is $\mathcal{M}_{6,6}(\mathbb{R})$ with all zeros except the entities:
 $b_{11} = \frac{1}{L}$, $b_{21} = \frac{2\dot{m}_H}{LA_H \rho_H}$, $b_{22} = \frac{A_H}{L} - \frac{\dot{m}_H^2(\frac{\partial \rho}{\partial P}|_H)_H}{LA_H \rho_H^2}$, $b_{23} =$
 $-\frac{\dot{m}_H^2(\frac{\partial \rho}{\partial h}|_P)_H}{LA_H \rho_H^2}$, $b_{33} = \frac{\dot{m}_H}{L}$, $b_{54} = -\frac{1}{L}$, $b_{55} = -\frac{2\dot{m}_C}{LA_C \rho_C}$, $b_{56} =$
 $-\frac{A_C}{L} + \frac{\dot{m}_C^2(\frac{\partial \rho}{\partial P}|_C)_C}{LA_C \rho_C^2}$, $b_{66} = -\frac{\dot{m}_C}{L}$.
- $C_1^S(x)$ is $\mathcal{M}_{6,6}(\mathbb{R})$ with all zeros except the entities:
 $c_{21} = f_H \frac{(2\dot{m}_H^2 + \epsilon)}{2A_H \rho_H \sqrt{\dot{m}_H^2 + \epsilon}} - 2\frac{\dot{m}_H \rho_{Hx}}{A_H \rho_H^2}$
 $c_{22} = -f_H \frac{\dot{m}_H \sqrt{\dot{m}_H^2 + \epsilon}(\frac{\partial \rho}{\partial P}|_H)_H}{2A_H \rho_H^2} - \frac{\dot{m}_H^2(\frac{\partial \rho}{\partial P}|_H)_H}{A_H \rho_H^2} +$
 $2\rho_{Hx} \dot{m}_H^2 \frac{(\frac{\partial \rho}{\partial P}|_H)_H}{A_H \rho_H^3}$
 $c_{23} = -f_H \frac{\dot{m}_H \sqrt{\dot{m}_H^2 + \epsilon}(\frac{\partial \rho}{\partial h}|_P)_H}{2A_H \rho_H^2} - \frac{\dot{m}_H^2(\frac{\partial \rho}{\partial h}|_P)_H}{A_H \rho_H^2} +$
 $2\rho_{Hx} \dot{m}_H^2 \frac{(\frac{\partial \rho}{\partial h}|_P)_H}{A_H \rho_H^3}$
 $c_{31} = (\frac{dH}{dx})_H$
 $c_{32} = \alpha \pi D_1 (\frac{\partial T}{\partial P}|_H)_H = -c_{63}$
 $c_{33} = \alpha \pi D_1 (\frac{\partial T}{\partial h}|_P)_H = -c_{64}$

$$c_{35} = -\alpha \pi D_1 (\frac{\partial T}{\partial P}|_h)_C = -c_{65}$$

$$c_{36} = -\alpha \pi D_1 (\frac{\partial T}{\partial h}|_P)_C = -c_{66}$$

$$c_{54} = f_C \frac{(2\dot{m}_C^2 + \epsilon)}{2A_C \rho_C \sqrt{\dot{m}_C^2 + \epsilon}} + 2\frac{\dot{m}_C \rho_{Cx}}{A_C \rho_C^2}$$

$$c_{55} = -f_C \frac{\dot{m}_C \sqrt{\dot{m}_C^2 + \epsilon}(\frac{\partial \rho}{\partial P}|_h)_C}{2A_C \rho_C^2} + \frac{\dot{m}_C^2(\frac{\partial \rho}{\partial P}|_h)_{Cx}}{A_C \rho_C^2} - 2\rho_{Cx} \dot{m}_C^2 \frac{(\frac{\partial \rho}{\partial P}|_h)_C}{A_C \rho_C^3}$$

$$c_{56} = -f_C \frac{\dot{m}_C \sqrt{\dot{m}_C^2 + \epsilon}(\frac{\partial \rho}{\partial h}|_P)_C}{2A_C \rho_C^2} + \frac{\dot{m}_C^2(\frac{\partial \rho}{\partial h}|_P)_{Cx}}{A_C \rho_C^2} - 2\rho_{Cx} \dot{m}_C^2 \frac{(\frac{\partial \rho}{\partial h}|_P)_C}{A_C \rho_C^3}$$

$$c_{62} = -(\frac{dH}{dx})_C$$

$(\frac{\partial \rho}{\partial P}|_h)_H$ is the partial derivative of density with respect to pressure at constant enthalpy for the hot flow. All other partial derivatives are interpreted in the same sense.

The the two matrices $A^S(x)$ and $B^S(x)$ in (12) are computed as: $A^S(x) = (A_1^S(x))^{-1} B_1^S(x)$ and $B^S(x) = (A_1^S(x))^{-1} C_1^S(x)$. Note that $A_1^S(x)$ is always invertible for flows of varying densities.

ACKNOWLEDGMENT

The authors are grateful to Virent Bhanot and Paolo Petagne (CERN) for their insights on the two phase process and model.

REFERENCES

- [1] B. Verlaat, M. Van Beuzekom, and A. Van Lysebetten, "CO2 cooling for HEP experiments," in *Topical Workshop on Electronics for Particle Physics (TWEPP-2008)*, Naxos, Greece, 2008, pp. 328–336.
- [2] G. Bastin and J.-M. Coron, *Stability and boundary stabilization of 1-d hyperbolic systems*. Springer, 2016, vol. 88.
- [3] D. Li, *Controllability and observability for quasilinear hyperbolic systems*. American Institute of Mathematical Sciences Springfield, Ill, USA, 2010.
- [4] R. Vazquez, M. Krstic, and J.-M. Coron, "Backstepping boundary stabilization and state estimation of a 2×2 linear hyperbolic system," in *50th IEEE Conference on Decision and Control and European Control Conference (CDC-ECC)*, 2011, pp. 4937–4942.
- [5] P. Bernard and M. Krstic, "Adaptive output-feedback stabilization of non-local hyperbolic PDEs," *Automatica*, vol. 50, no. 10, pp. 2692–2699, 2014.
- [6] L. Hu, F. Di Meglio, R. Vazquez, and M. Krstic, "Control of homodirectional and general heterodirectional linear coupled hyperbolic PDEs," *IEEE Transactions on Automatic Control*, vol. 61, no. 11, pp. 3301–3314, 2016.
- [7] J. Auriol and F. Di Meglio, "Minimum time control of heterodirectional linear coupled hyperbolic PDEs," *Automatica*, vol. 71, pp. 300–307, 2016.
- [8] F. Castillo, E. Witrant, C. Prieur, and L. Dugard, "Boundary observers for linear and quasi-linear hyperbolic systems with application to flow control," *Automatica*, vol. 49, no. 11, pp. 3180–3188, 2013.
- [9] F. Zobiri, E. Witrant, and F. Bonne, "PDE observer design for counter-current heat flows in a heat-exchanger," *published*, 2017.
- [10] P.-O. Lamare, A. Girard, and C. Prieur, "An optimisation approach for stability analysis and controller synthesis of linear hyperbolic systems," *ESAIM: Control, Optimisation and Calculus of Variations*, vol. 22, no. 4, pp. 1236–1263, 2016.
- [11] G. P. Peterson, "An introduction to heat pipes: modeling, testing, and applications," 1994.
- [12] B. Bradu, P. Gayet, S.-I. Niculescu, and E. Witrant, "Modeling of the very low pressure helium flow in the lhc cryogenic distribution line after a quench," *Cryogenics*, vol. 50, no. 2, pp. 71–77, 2010.